

## Quantifying the sensitivity of simulated climate change to model configuration

Barry H. Lynn · Richard Healy · Leonard M. Druyan

Received: 25 September 2006 / Accepted: 1 August 2008 / Published online: 17 September 2008  
© Springer Science + Business Media B.V. 2008

**Abstract** This study used “factor separation” to quantify the sensitivity of simulated present and future surface temperatures and precipitation to alternative regional climate model physics components. The method enables a quantitative isolation of the effects of using each physical component as well as the combined effect of two or more components. Simulation results are presented from eight versions of the Mesoscale Modeling System Version 5 (MM5), one-way nested within one version of the Goddard Institute for Space Studies Atmosphere–Ocean Global Climate Model (GISS AOGCM). The MM5 simulations were made at 108 km grid spacing over the continental United States for five summers in the 1990s and 2050s. Results show that the choice of cumulus convection parameterization is the most important “factor” in the simulation of contemporary surface summer temperatures and precipitation over both the western and eastern USA. The choice of boundary layer scheme and radiation package also increases the range of model simulation results. Moreover, the alternative configurations give quite different results for surface temperature and precipitation in the 2050s. For example, simulated 2050s surface temperatures by the scheme with the coolest 1990s surface temperatures are comparable to 1990s temperatures produced by other schemes. The study analyzes the spatial distribution of 1990s to 2050s projected changes in the surface temperature for the eight MM5 versions. The predicted surface temperature change at a given grid point,

---

B. H. Lynn  
Department of Earth Sciences, Hebrew University of Jerusalem and Weather It Is, Ltd.,  
Efrat, Israel

R. Healy  
Woods Hole Oceanographic Institute, Woods Hole, MA 02543, USA

L. M. Druyan  
Columbia University, Center for Climate Systems Research, New York, NY 10025, USA

L. M. Druyan (✉)  
NASA/Goddard Institute for Space Studies, 2880 Broadway, New York, NY 10025, USA  
e-mail: LDruyan@giss.nasa.gov

averaged over all eight model configurations, is generally about twice the standard deviation of the eight predicted changes, indicating relative consensus among the different model projections. Factor separation analysis indicates that the choice of cumulus parameterization is the most important modeling factor amongst the three tested contributing to the computed 1990s to 2050s surface temperature change, although enhanced warming over many areas is also attributable to synergistic effects of changing all three model components. Simulated ensemble mean precipitation changes, however, are very small and generally smaller than the inter-model standard deviations. The MM5 versions therefore offer little consensus regarding 1990s to 2050s changes in precipitation rates.

## 1 Introduction

Regional climate models have been used to downscale global climate model (GCM) output in order to better focus on the spatial details of regional climate change (e.g., Dickinson et al. 1989; Bates et al. 1993; Giorgi et al. 1993a, b, 1994; Walsh and McGregor 1995; Nobre et al. 2001; Bell et al. 2004; Han and Roads 2004; Leung et al. 2004; Liang et al. 2004; Fu et al. 2005; Diffenbaugh et al. 2005; Lynn et al. 2004, 2006; Gao et al. 2006). Regional models can improve the representation of local meteorology for climate change impact studies because they employ higher grid resolution than GCMs, and also better resolve convective-scale processes, topographically driven circulations, and air-sea contrasts leading to sea-breezes circulations (Giorgi and Marinucci 1996; Colle et al. 2000; Mass et al. 2002; Leung and Qian 2003; Leung et al. 2003a, b, c).

Cortinas and Stensrud (1995) and Rosenzweig and Solecki (2001) suggested that it would be useful to test the sensitivity of simulated climate change to model physics configurations of regional atmospheric models used in local climate change impact studies. Han and Roads (2004) compared results from a regional model at different horizontal resolutions (but the same model physics parameterizations) to results from a GCM with different model physics, which was used to force the regional-scale model. They found that grid resolution differences for the regional model did not have a large impact on the simulations. On the other hand, there were important differences between regional model simulation results and the GCM product, which were attributed to differences to model physics. Giorgi (2006) also identified the choice of model physics configuration as a factor in creating uncertainty in evaluating future climate change scenarios, and suggested that probability distribution functions (pdfs) of future climate be constructed to better quantify this uncertainty. Yang and Arritt (2002) used ranges of plausible values for two parameters in the deep convection scheme of the RegCM2 and evaluated the consequences to two 60-day regional climate simulations over the central USA. They varied the timescale for release of convective instability through a range of five values from 600 to 7,200 s, and the maximum stable-layer depth between updraft origin and the level of free convection over five values from 50 to 150 mb, to create 25-member ensembles. They found that the ensemble mean had superior skill to the reference forecast, which used the default values of the closure parameters, but in one of the two cases, this skill was not superior to climatology. The Yang and Arritt study attempted to circumvent uncertainties in the convection scheme by generating ensemble results covering the

**Table 1** List of acronyms for the eight model configurations

List of acronyms	Boundary layer scheme	Cumulus parameterization	Radiation package
MIBR	MRF	Betts–Miller	RRTM
EBR	Eta	Betts–Miller	RRTM
MIGR	MRF	Grell	RRTM
MIBC	MRF	Betts–Miller	CCM2
MIGC	MRF	Grell	CCM2
EGR	Eta	Grell	RRTM
EBC	Eta	Betts–Miller	CCM2
EGC	Eta	Grell	CCM2

Boundary layer schemes: Medium Range Forecast Model (*M*, *MRF*) or Eta (*E*); cumulus parameterizations Betts–Miller (*B*) or Grell (*G*); radiation packages: Community Climate Model version 2 (*C*, *CCM2*) or Rapid Radiation Transfer Model (*R*, *RRTM*). MIBR, MIGR, MIBC and MIGC schemes include turbulent mixing in clouds

entire range of possibilities. The present study is motivated by the broader objective to test and document the sensitivity of regional simulations of temperature and precipitation rates to eight different combinations of alternative model component schemes.

In this study simulated winds, temperatures, humidities and sea-surface temperatures from the Goddard Institute for Space Studies Atmosphere–Ocean Global Climate Model (GISS AOGCM) (Hansen et al. 2002; Russell et al. 1995) are used to force the Mesoscale Modeling System, Version 5 (MM5) (Dudhia 1993; Grell et al. 1994). The MM5 was initialized with AOGCM soil moisture and temperatures. Results from the modeling system were previously used in an interdisciplinary study of climate change and land-use change on regional climate, air quality, and health in the New York Metropolitan Region, the New York Climate and Health Project (Hogrefe et al. 2004; Knowlton et al. 2004; Bell et al. 2007). In these studies, the main emphasis was on air quality and pollution results were obtained primarily with a single model configuration. We perceived the need to quantitatively evaluate the relative sensitivity of simulation results to components of the model physics as well as the climate change forcing. Specifically, this paper analyzes the sensitivity of the MM5's present and future simulated surface temperatures and precipitation to eight combinations of each of three model physics components: cumulus parameterization, boundary layer scheme and radiation package, all described in Section 2.2 and summarized in Table 1.

## 2 Model descriptions

### 2.1 GISS AOGCM

Lateral boundary and initial conditions for the MM5 were taken from the GISS AOGCM, which has been extensively used in climate sensitivity studies. The version used here is a coupled atmosphere–ocean version with horizontal grid spacing of 4° by 5° (Russell et al. 1995). Computations were made for nine vertical atmospheric layers and 12 vertical ocean layers with realistic bathymetry. Results for the 1990s and the 2050s were taken from the GISS AOGCM forced by the IPCC SRES A2

scenario of greenhouse gas and sulfate emissions trends (IPCC 2000), which account for the effects of volcanic aerosols in the 1990s (Sato et al. 1993).

## 2.2 MM5

The non-hydrostatic Mesoscale Modeling System, Generation 5, MM5 version 3.6 (Dudhia 1993; Grell et al. 1994), developed at Pennsylvania State University and the National Center for Atmospheric Research, was nested within the GISS AOGCM. The standard model includes predictions for the three-dimensional wind components, temperature, mixing ratios for water vapor, and cloud water/ice and rain/snow (using bulk parameterizations).

MM5 lower boundary conditions are calculated by the land surface model of Chen and Dudhia (2001a, b). This model contains interactive soil and vegetative layers, and calculates a surface energy balance for the combined ground vegetation surface. It incorporates a coupling of the diurnally dependent Penman potential evaporation approach of Mahrt and Ek (1984), the multilayer soil model of Mahrt and Pan (1984), and the primitive canopy model of Pan and Mahrt (1987). Chen et al. (1996) extended it to include the modestly complex canopy resistance approach of Noilhan and Planton (1989) and Jacquemin and Noilhan (1990). It has one canopy layer and prognosticates the following variables: soil moisture and temperature in the soil layers, water stored on the canopy, and snow stored on the ground. The soil model uses four soil layers, and the thickness of each layer from the ground surface to the bottom are 0.1, 0.3, 0.6, and 1.0 m, respectively. The total soil depth is 2 m, with the root zone in the upper 1 m of soil. The lower 1-m soil layer acts like a reservoir with a gravity drainage at the bottom.

The present study focuses on the performance of the following MM5 components: (1) the planetary boundary layer (PBL) scheme, (2) the cumulus parameterization, and (3) the radiation package. We tested two options for each category: (1) the Medium Range Forecast Model (MRF) versus Eta planetary boundary layer scheme; (2) the Betts–Miller versus Grell cumulus parameterization; (3) the Community Climate Model (CCM2) versus the Rapid Radiative Transfer Model (RRTM) radiation package. The boundary layer, cumulus and radiation parameterizations are all widely used in mesoscale modeling studies and are designed to work at the spatial scales considered in the current research.

The MRF PBL is an efficient scheme based on the Troen–Mahrt representation of the counter-gradient term and K profile in the well-mixed PBL (Hong and Pan 1996). The MRF also includes vertical mixing in clouds, i.e., mixing along a wet adiabat. In comparison, the Eta PBL is based on the Mellor–Yamada scheme that predicts the turbulent kinetic energy (TKE). It uses the TKE to affect local mixing and does not include vertical mixing in clouds (Janjic 1990, 1994).

The Betts–Miller moist convection scheme is based on a relaxation adjustment to a reference post-convective thermodynamic profile over a given period (Betts 1986; Betts and Miller 1986, 1993; Janjic 1994). In comparison, Grell uses the quasi-equilibrium assumption of Arakawa and Schubert (Grell et al. 1991; Grell 1993). In this scheme, the rate of cloud stabilization associated with moist convection balances the large-scale destabilization rate. Lynn et al. (2004) applied a modification, also used here, that allows the Grell scheme to produce afternoon convection in the southeast more consistent with the observed timing of precipitation.

The CCM2 radiation scheme accounts for multiple short-wave and spectral bands. It includes the effects of both resolved and unresolved clouds (based on a relative humidity-derived cloud fraction (Hack et al. 1993)). The RRTM contains both short-wave and long-wave radiation transfer schemes (Mlawer et al. 1997), but does not include a relative humidity-derived cloud fraction.

The eight MM5 versions used in the study incorporate different combinations of the aforementioned model components as shown in Table 1.

### 3 Methods

Factor separation analysis (Stein and Alpert 1993) was used to quantify the contributions to changes in a particular output variable that result from changing the model configuration. The model sensitivity to three model configuration “factors” was tested. The three factors were (1) the choice of boundary layer scheme, (2) the choice of cumulus parameterization, and (3) the choice of radiation transfer scheme. The alternative schemes were described in Section 2 and the equations used to compute the model sensitivity to the factors are given in Appendix. The analysis identifies contributions from both individual, coupled and/or synergistic changes to the model parameterizations. The experiments summarized in Table 1 were designed to supply the appropriate data for the factor analysis. For example, MIBR and EBR differ only in the boundary layer scheme, MIBR and MIGC differ in both the convection and radiation schemes, and MIBR and EGC differ with regard to all three components.

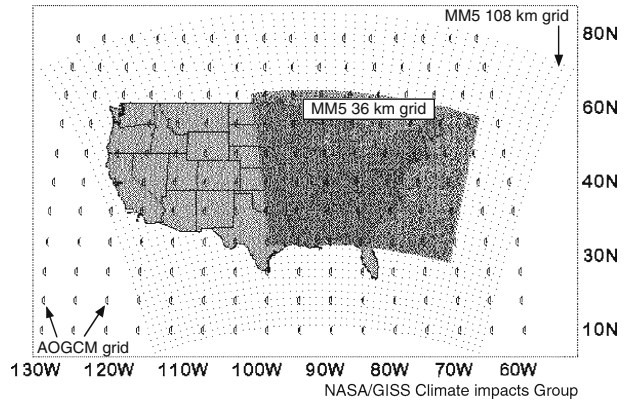
#### 3.1 Coupling

The one-way nesting of the MM5 model uses GISS AOGCM data for initialization and subsequently for lateral boundary conditions. Six-hourly GISS AOGCM data were interpolated to the lateral boundaries of the higher-resolution, MM5 grid. A five-point linear time interpolation was used to make the lateral boundary data synchronous with MM5 time steps, following Davies and Turner (1977). Sea-surface temperatures computed by the GISS AOGCM formed the lower boundary conditions over water. The land surface model was initialized at the first time step with GISS AOGCM soil temperature and soil moisture, interpolated to the MM5 grid. In one experiment described in Section 4.3, the MM5 was also driven with observed NCEP reanalysis data (instead of AOGCM data) for the summer of 1993.

#### 3.2 Simulation experiments

The study used a continuous GISS AOGCM simulation between 1990–2057, based on the IPCC A2 scenario of increasing atmospheric concentrations of greenhouse gases and sulfate emissions. Results are presented for MM5 simulations during five summers in the 1990s and the 2050s, respectively, which were driven by the June–August 1990s and 2050s portions of the AOGCM multi-decadal simulation. Note that the study does not consider continuous 60-year MM5 simulations. Downscaling only brief excerpts of the AOGCM results is often called “time-slice mode.” Most of the simulations with the MM5 model were run at 108 km resolution within a domain

**Fig. 1** A schematic of model grid domains: GISS AOGCM  $4^\circ \times 5^\circ$ ; MM5 108 and 36 km. The 108 km grid's western and eastern boundaries ( $132^\circ$  W and  $42^\circ$  W, respectively) were configured well over the Pacific and Atlantic Oceans to minimize adverse boundary effects



that covered the continental USA. Figure 1 shows the MM5 108 grid superimposed on the GISS AOGCM grid. The 108 km grid's western and eastern boundaries ( $132^\circ$  W and  $42^\circ$  W, respectively) were configured well over the Pacific and Atlantic Oceans to minimize adverse boundary effects. Regional mesoscale models are typically run at grid resolutions higher than 108 km, especially for local impact studies. In this case, however, running the MM5 on the 108 km grid facilitated the large number of simulations needed to provide statistically significant results. Accordingly, the sensitivity of model results to grid-resolution was tested in one set of double-nesting experiments, in which the 108 km grid domain results forced an inner simulation on a 36 km grid over the eastern USA (see also Fig. 1). The sensitivity tests of horizontal grid resolution (Section 4.3) were done for MIBR and EGC, the two versions that had none of the three model physics components in common.

The MM5 was run with thirty-five vertical layers, including finer vertical resolution in the lower troposphere to allow the model to better simulate boundary-layer processes. The time step was 270 s (90 s for the 36 km grid of the nested runs), and each simulation was run from May 1st to Sept 1st. MM5 soil temperature and soil moisture distributions were initialized from the GISS AOGCM. Starting the model in May allowed the atmospheric and surface condition components of the regional model time to 'spin-up,' before the start of the study period on June 1st of each summer, since soil moisture and temperature evolve in response to radiation, wind, and precipitation forcing. Atmospheric concentrations of  $\text{CO}_2$  in the MM5 were synchronized with those prescribed for the GISS AOGCM.

Section 4.1 discusses the validation of MM5 1990s simulations for the different model versions and the sensitivity of simulated surface air temperature and precipitation to the several alternative model formulations. Section 4.2 discusses the models' projections of 2050s climate and the consequences of the sensitivities for climate change experiments. Section 4.3 describes tests of simulations' sensitivities to the number of seasons, to the differences between AOGCM and reanalysis forcing and to models' horizontal resolution.

### 3.3 Validation

MM5 mean temperature and precipitation rates for June to August 1993–1997 from the 108 km and 36 km grids were validated against corresponding hourly airways

**Table 2** JJA 1993–1997 area mean surface temperatures ( $^{\circ}\text{C}$ ) and downward radiation ( $\text{W m}^{-2}$ ) at the Earth's surface

OBS	MIBR	EBR	MIGR	MIBC	MIGC	EGR	EBC	EGC
Surface air temperature – West								
22.25	21.49	19.55	19.56	19.58	18.46	17.85	17.93	17.03
Surface air temperature – East								
22.31	24.68	23.34	21.01	22.68	20.55	18.46	18.74	18.26
Downward long wave radiation at Earth's surface – West								
<sup>a</sup>	354	<sup>a</sup>	359	327	337	361	333	345
Downward long wave radiation at Earth's surface – East								
<sup>a</sup>	392	<sup>a</sup>	389	372	381	391	383	388
Downward short wave radiation at Earth's surface – West								
263 <sup>b</sup>	266	274	231	267	238	211	249	207
Downward short wave radiation at Earth's surface – East								
245 <sup>b</sup>	226	228	169	232	167	122	150	120

*OBS* Observed; other acronyms as in Table 1

<sup>a</sup>Data not available

<sup>b</sup>1990–1999 averages, based on Darnell et al. (1996)

station observations over the USA and Canada for about 1,000 stations, obtained from the NCAR mass storage system. To facilitate the validation, these data were spatially interpolated to the MM5 grid. MM5 means of incident solar radiation were validated against corresponding data from the Langley Observatory (Darnell et al. 1996).

## 4 Results

### 4.1 JJA 1993–1997

Tables 2 and 3 show that the various MM5 configurations produced a wide range of temperatures, surface radiation fluxes and precipitation amounts for the western and eastern USA. No particular model configuration “stands-out” as being better than another over the whole continental USA, although the model configuration MIBR produced fairly good agreement between simulated and observed average temperature in the western USA (Table 2). MIBC, which shares the same convection and PBL schemes, simulated the most realistic surface temperatures in the eastern USA. The area temperatures over the eight experiments are positively correlated with the corresponding downward short wave radiation received at the Earth's

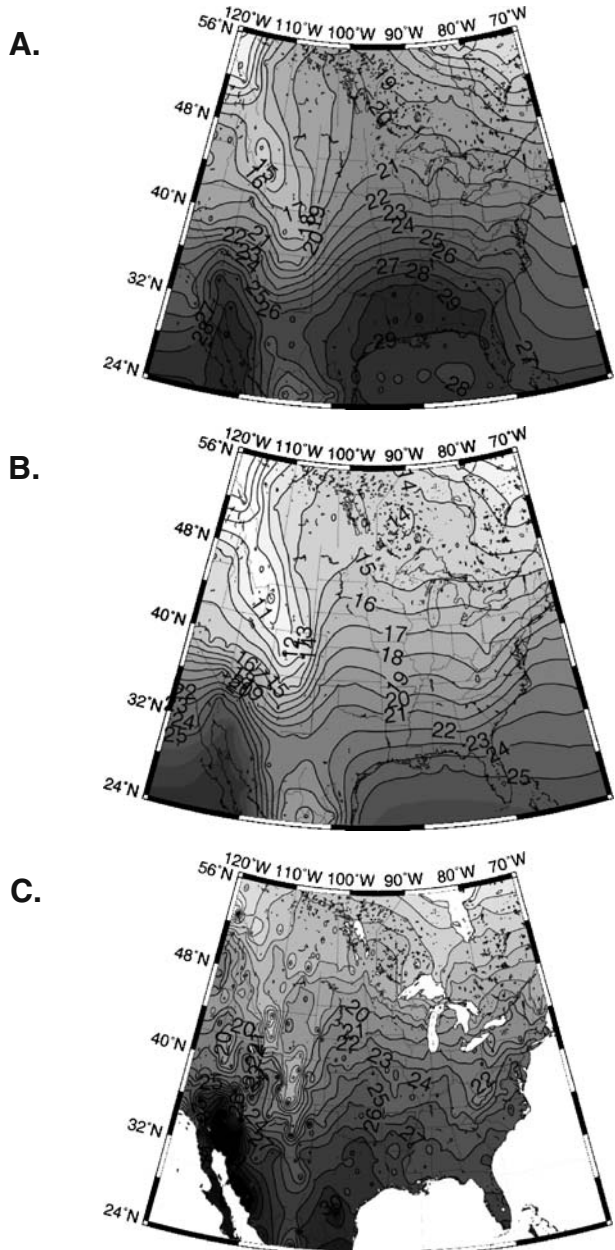
**Table 3** JJA 1993–1997 area mean precipitation accumulation (mm)

	OBS	MIBR	EBR	MIGR	MIBC	MIGC	EGR	EBC	EGC
West									
JJA 1993–97	108.35	228.9	209.3	149.2	169.4	153.0	169.8	195.7	167.2
East									
JJA 1993–97	243.0	391.8	366.4	279.1	354.1	289.4	187.1	303.1	207.6

*OBS* Observed; other acronyms as in Table 1

surface, with coefficients 0.74 in the west and 0.95 in the east. The model versions with the lowest temperatures underestimated the seasonal mean of the incident downward short wave radiation compared with observations. All of the experiments were too rainy compared with observations in the western USA, and six of the

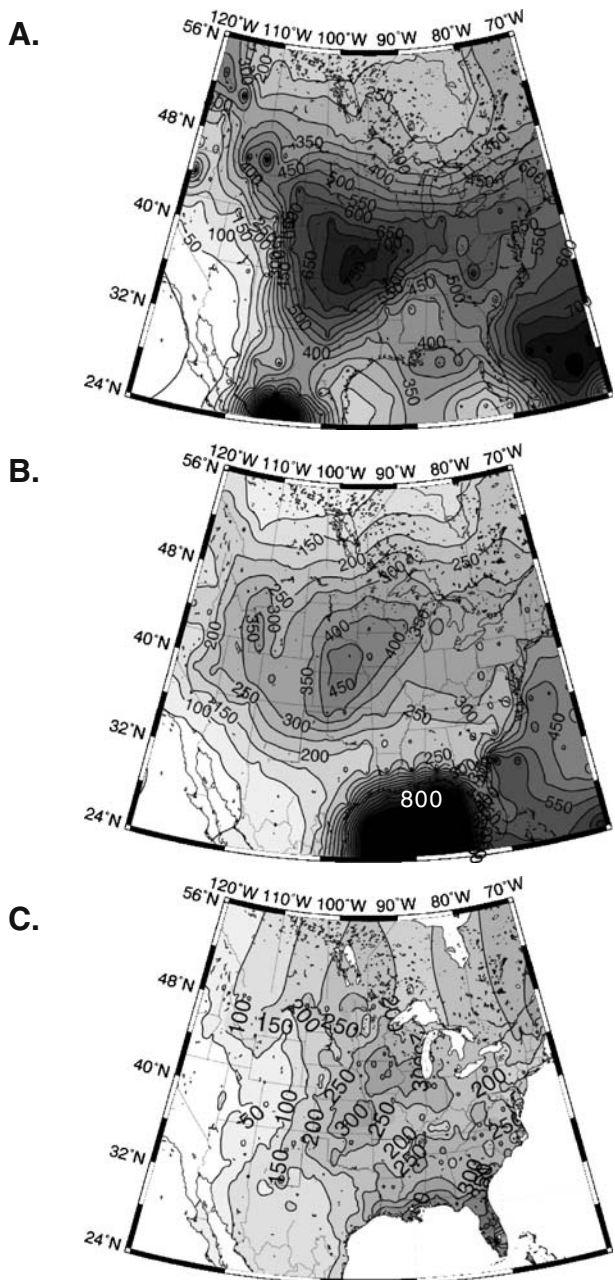
**Fig. 2** Simulated surface temperatures averaged over JJA 1993–1997. **a** MIBR, **b** EGC, **c** observed



eight were too rainy in the east. MIGR achieved the most realistic precipitation considering both areas, with EGC a close second best.

Figure 2 illustrates the spatial distribution of surface temperatures from the warmest and wettest (MIBR) and coolest and (one of the) driest (EGC) simulations

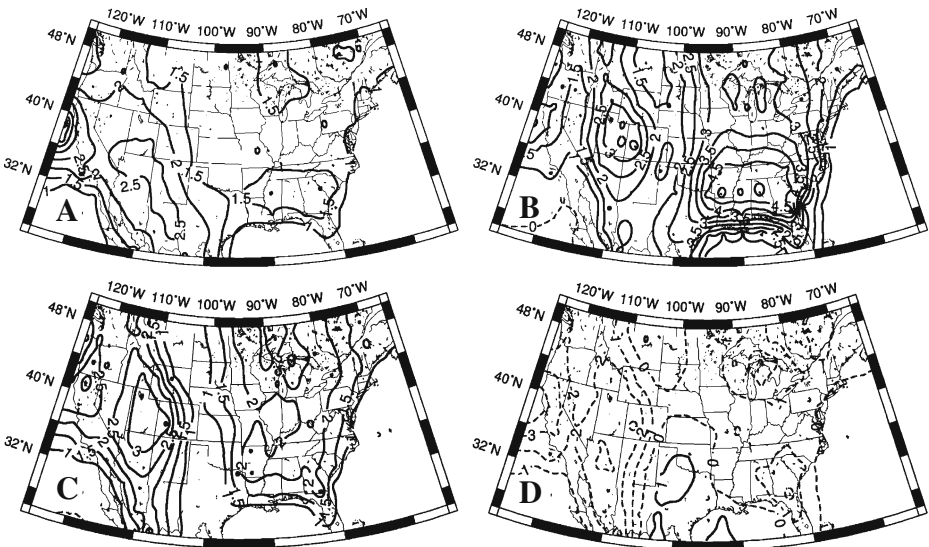
**Fig. 3** Simulated JJA precipitation accumulations averaged over 1993–1997. **a** MIBR, **b** EGC, **c** observed



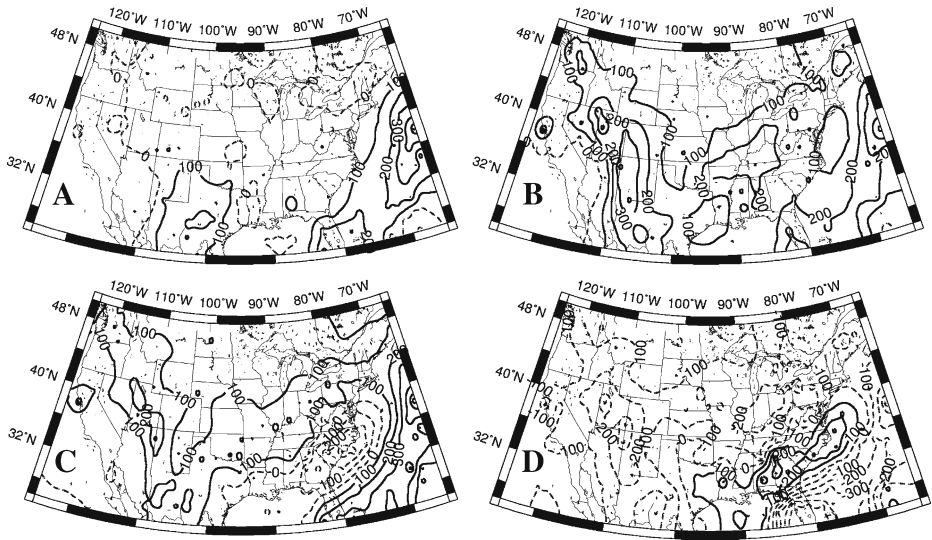
for JJA 1993–1997 across the contiguous USA. In some locations, these MIBR mean 1990s surface temperatures were as much as 8°C warmer than corresponding EGC temperatures. Over land, they were several hundred mm rainier as well (Fig. 3). Hence the range of differences between models is comparable to commonly expected climate change differences over future decades. Comparison with the observed field (Fig. 2c) shows the MIBR distribution to be the more realistic of the two.

Figure 3 shows the horizontal distributions of simulated JJA 1993–1997 precipitation rates from MIBR and EGC and compares them to observations. The results do not compare well with the observed precipitation distribution (Fig. 3c). For example, while EGC is reasonable over the Midwest, it simulates excessive rainfall over the Gulf of Mexico. The MIBR, on the other hand, produced higher and less realistic precipitation rates compared to EGC over much of the eastern two-thirds of the USA.

Figure 4 shows the results of the Stein and Alpert (1993) factor separation technique, used here to evaluate the singular and coupled (synergistic) contributions of each tested model component on the simulation of JJA 1993–1997 surface air temperatures. Specifically, results quantify the consequences of the modeling choices for boundary layer scheme, cumulus convection parameterization, and radiation package. Figure 4a shows somewhat higher 1990s surface temperature as the consequence of using the MRF boundary layer scheme in place of the Eta scheme. Figure 4b shows a stronger increase in surface temperatures, especially in the southeastern USA, as a consequence of using the Betts–Miller moist convection



**Fig. 4** Factor separation results for MM5 simulated JJA 1993–1997 surface air temperature. **a** The contribution of changing the boundary layer scheme from Eta to MRF (when using the Betts–Miller cumulus parameterization and RRTM radiation package). **b** The contribution of using the Betts–Miller instead of Grell cumulus parameterization (when using the MRF and RRTM). **c** The contribution of changing the radiation package from CCM2 to RRTM (when using the MRF and Betts–Miller). **d** The contribution of coupled and synergistic terms that arise among the various combinations when all factors are changed. Units: °C



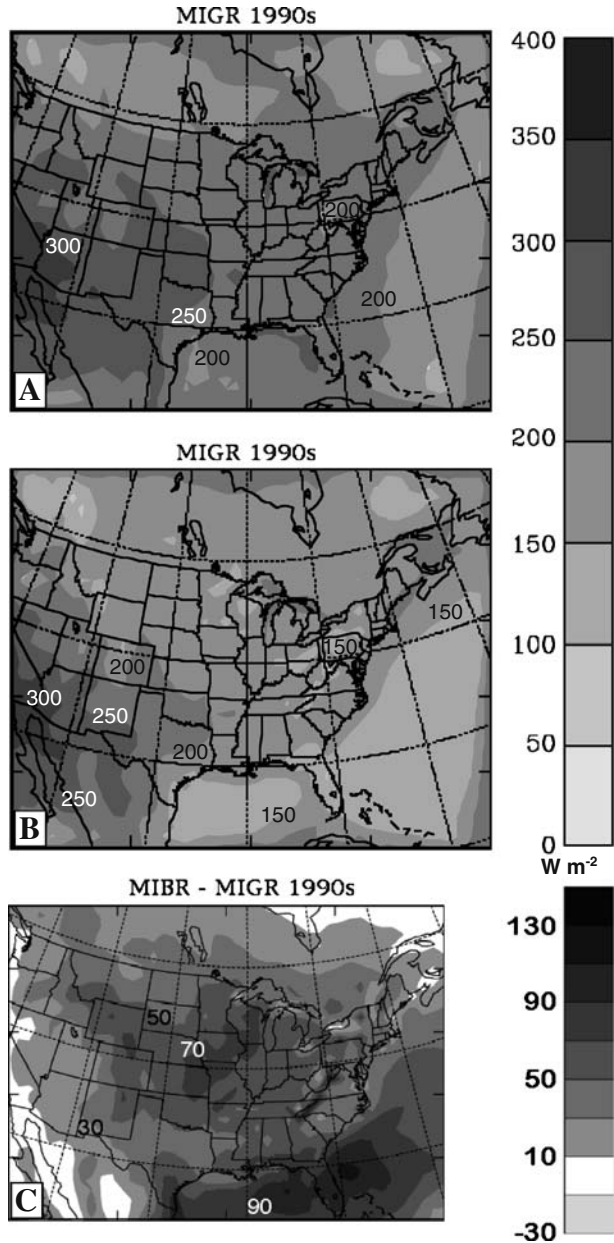
**Fig. 5** Same as Fig. 4, but for accumulated precipitation. Units: mm

scheme instead of the Grell scheme. Figure 4c shows that using the RRTM radiation scheme instead of the CCM2 radiation package also increased surface temperatures, except for a swath along the eastern slopes of the Rocky Mountains. The coupled or synergistic contributions to temperature, mapped in Fig. 4d, quantify the impacts not accounted for by any of the individual changes attributable to each of the single factors. Changing two or more factors can produce impacts that the individual factors do not produce alone. These synergistic effects on surface temperatures, shown in Fig. 4d, mostly indicated cooling, but they were relatively small compared to the impacts of the individual factors themselves.

Figure 5 shows the results of factor separation for accumulated precipitation. The MRF produced more precipitation than the Eta over the Southern and Central Plains (Fig. 5a). The choice of cumulus parameterization produced the greatest increase in precipitation rates (Fig. 5b) compared to the other factors. Using Betts–Miller instead of Grell increased simulated precipitation amounts in the eastern two-thirds of the USA. Using RRTM instead of CCM2 also increased precipitation in many locations (Fig. 5c). The synergistic effects of the three alternative components (Fig. 5d) gave large decreases in precipitation over most of the USA, but they nevertheless account for some of the excessive Gulf of Mexico precipitation in the EGC experiment (compare Fig. 3b, c).

Figure 6 shows the JJA 1993–1997 average of surface incident shortwave radiation from MIBR and MIGR, a diagnostic that helps explain the influence that the choice of cumulus parameterization has on surface temperatures. MIBR simulated mean values of incoming shortwave radiation that were much closer to observations (not shown). Higher surface temperatures associated with more incoming radiation (Fig. 6c) were more consistent with the triggering of deeper moist convection, leading to more precipitation with Betts–Miller than Grell. However, the predominance of convective precipitation in MIBR allows for more frequent rainless periods

**Fig. 6** The JJA 1993–1997 averages of downward shortwave radiation flux at the ground surface in the **a** MIBR experiment, **b** MIGR experiment, **c** MIBR minus MIGR

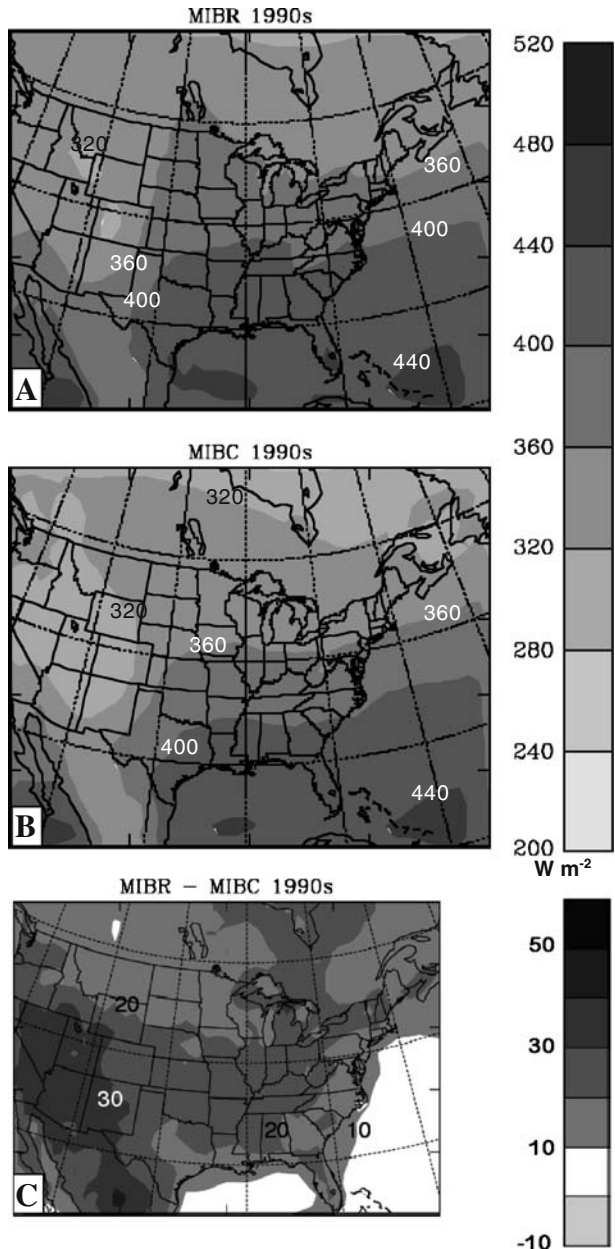


compared with the MIGR simulation, which simulated much light non-convective precipitation, too frequently (see Lynn et al. 2006 for more details). The temperature differences between MIGR and MIBR were also amplified by differences in the timing of precipitation: MIBR produced peak precipitation overnight while MIGR produced precipitation maxima during the day (in the Southeast USA). Lynn et al. (2004) found that activation of the convective triggers in the Grell scheme

produces more daytime moist convection than the Betts–Miller scheme (for the same conditions). Initiation of convection in the Betts–Miller scheme requires large-scale destabilization, which often occurs overnight over the eastern USA.

Figure 7 shows the JJA 1993–1997 averages of surface incident long wave radiation from the MIBR and MIBC experiments, which differ only in their treatment of

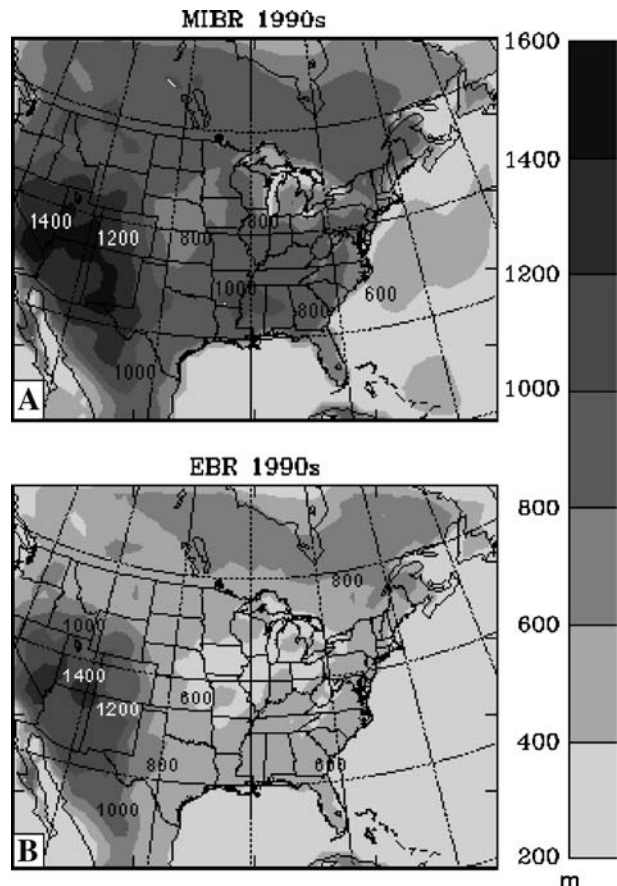
**Fig. 7** The JJA 1993–1997 averages of downward long wave radiation flux at the ground surface in the **a** MIBR experiment, **b** MIBC experiment, **c** MIBR minus MIBC



radiation transfer (see Table 1). The MIBR simulation (which uses RRTM) generally experienced greater downward fluxes of long wave radiation incident at the surface (Fig. 7c), although the two experiments gave similar amounts of shortwave energy (Table 2). This excess long wave energy is consistent with the relatively higher temperatures of the RRTM (Table 2).

Figure 8 shows the JJA 1993–1997 means of the daily maximum height of the planetary boundary layer for the MIBR and EBR experiments, which differ only in the choice of their respective boundary layer schemes (MRF versus Eta). Figure 4 shows that the choice of the MRF over the Eta scheme contributed to higher JJA 1993–1997 surface temperatures. Nevertheless, shortwave radiation flux reaching the ground was not much different in MIBR than in EBR (not shown). Figure 8 shows that MIBR produced higher maximum boundary layer heights over many areas, and especially in the mountainous western region, where the choice of boundary layer scheme has its largest effect on surface temperatures. We note that the MRF includes both local and non-local closure parameterizations, whereas the Eta scheme includes only a local closure scheme. Non-local closure allows more rapid and deeper mixing within MIBR's deeper boundary layer. This promotes higher fluxes of sensible heat

**Fig. 8** The JJA 1993–1997 averages of daily maximum planetary boundary layer height in the **a** MIBR and **b** EBR experiments

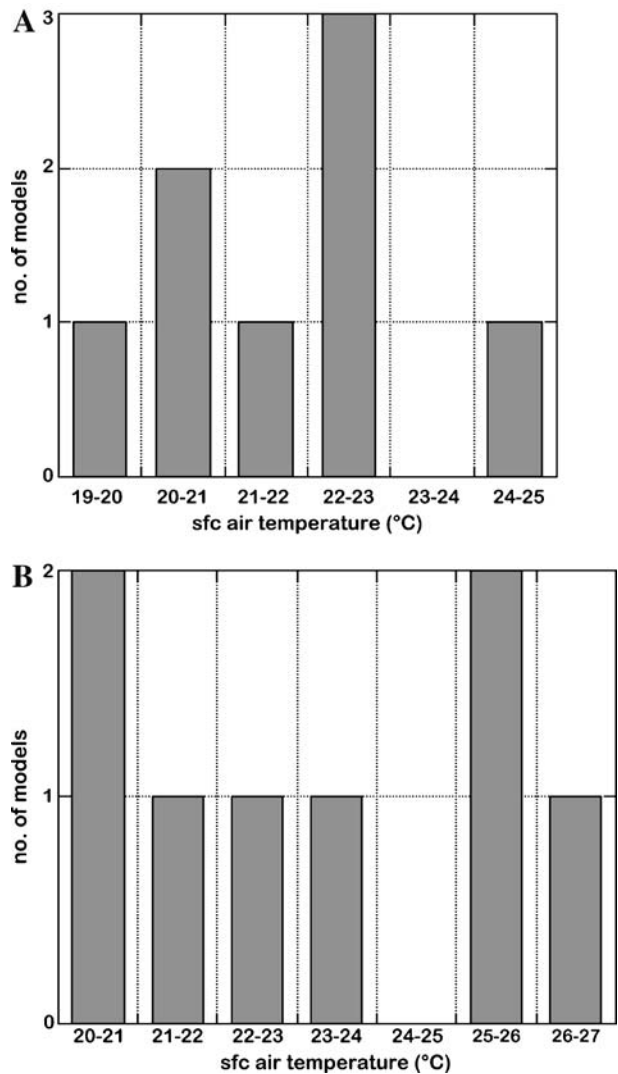


(and moisture) from the ground surface, raising surface temperatures and triggering moist convection. Indeed, JJA 1993–1997 mean sensible heat fluxes for MIBR were generally larger over most of the continental USA than for EBR (not shown).

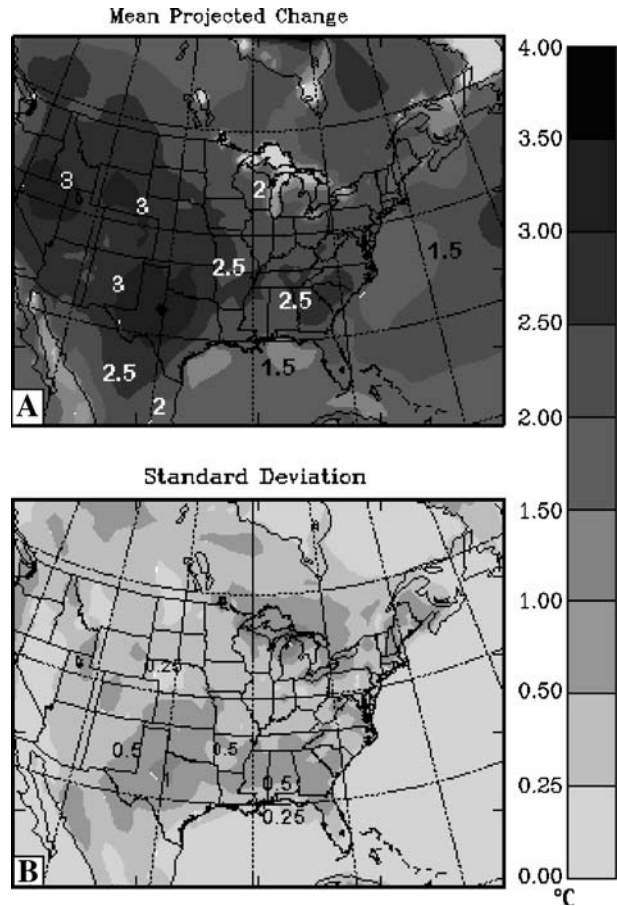
#### 4.2 Simulated climate change

Figure 9a, b show, for the western and eastern United States, respectively, frequency distributions of the different JJA 2053–2057 regional mean surface temperatures ( $T_s$ ) simulated by the different MM5 model experiments. Three of the models simulate a mean temperature between 22°C and 23°C over the western USA, but the range between the warmest and coolest versions was 5°C. Over the Eastern USA, the

**Fig. 9** Histograms of area mean temperature projected for JJA 2053–2057, for the eight model configurations described in Table 1. **a** Western USA, **b** Eastern USA



**Fig. 10** **a** Projected 1990s to 2050s changes in JJA surface temperatures, averaged over the eight model experiments. **b** The standard deviation of the changes in surface temperature between the eight experiments



scatter of the results was even greater, and the range between the warmest and coolest versions was 6°C. Six of the eight model configurations simulated mean JJA 2053–2057 precipitation amounts within the western USA of between 150 and 200 mm, and the other two between 200–250 mm (not shown). However, over the eastern United States the dispersion of the simulated mean JJA 2053–2057 precipitation amounts among the model versions was much larger (not shown). The model configurations with higher temperatures and higher precipitation rates in the 1990s also projected the highest temperatures and the rainiest regimes for the 2050s.

Figure 10a shows the simulated 1990s to 2050s changes in JJA surface temperatures, averaged over the eight model experiments and Table 4 gives their spatial means for each experiment over the eastern and western USA. Figure 10b shows the spatial distribution of standard deviations (SD) between the eight projections at each grid point. The largest temperature changes are within the Western States, with maxima over the Great Basin and the lower Great Plains. At most locations, the mean change is more than two SD, suggesting a “consensus” for the projected temperature trends between the model versions. The smaller the standard deviations based on the eight experiments, the closer in value are the eight projections of surface

**Table 4** Area averaged changes in surface temperature ( $\Delta T$ ,  $^{\circ}\text{C}$ ) and precipitation rate ( $\Delta\text{Pr}$ , mm), 2050s minus 1990s, for each experiment

Experiment	MIBR	EBR	MIGR	MIBC	MIGC	EGR	EBC	EGC
$\Delta T$ , West	2.87	2.87	2.63	3.12	2.68	2.53	2.90	2.65
$\Delta T$ , East	1.99	2.60	2.07	2.89	2.22	2.35	2.28	2.32
$\Delta\text{Pr}$ , East	-30.6	39.8	22.4	29.6	23.5	22.2	45.4	17.4
$\Delta\text{Pr}$ , West	-28.1	10.9	32.6	44.2	31.0	16.1	35.0	25.1

temperature changes to each other. “Consensus” here means that the ensemble mean temperature change is much more different from zero than most of the individual changes are different from each other. The small spread between the area averages of temperature change given in Table 4 reflects this consensus. On the other hand, projected mean changes in precipitation (Table 4) are relatively small and, moreover, generally lower than the standard deviations between results from the eight model projections, indicating great uncertainty. In fact, there is even uncertainty in the sign of the simulated changes in mean precipitation.

Figure 11 shows results of factor separation analysis evaluating the contributions of the alternative model components to the MM5 simulations of 1990s to 2050s changes in surface air temperatures. Results show that the MM5’s temperature change projections (in time slice mode) over the southern Plains are made warmer by the Betts–Miller convection scheme, the MRF PBL and to a lesser extent by

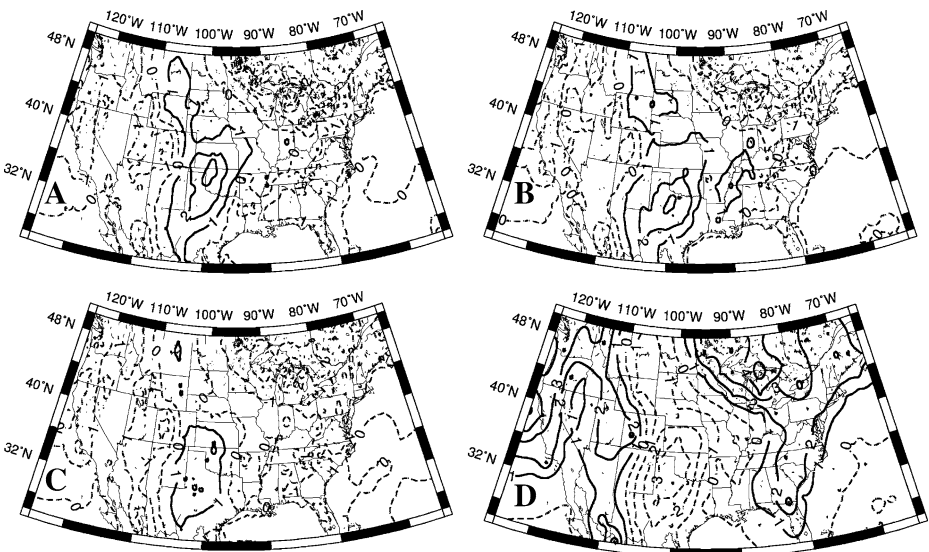


**Fig. 11** Factor separation analysis results showing the impact of three model components on MM5 simulated 1990s to 2050s changes in surface air temperatures. **a** The impact of changing the boundary layer scheme from Eta to MRF (when using the Betts–Miller cumulus parameterization and RRTM radiation package). **b** the impact of using the Betts–Miller instead of Grell cumulus parameterization (when using the MRF and RRTM). **c** the effect of changing the radiation package from CCM2 to RRTM (when using the MRF and Betts–Miller). **d** the effect of coupled and synergistic terms that arise among the various combinations when all factors are changed. Units:  $^{\circ}\text{C}$

**Table 5** Statistical comparison of eight- model ensemble mean JJA 1993 MM5 temperature and precipitation results from simulations over the continental USA forced with alternative AOGCM or NCEP reanalysis

Model	T (°C)	$\sigma_T$ (°C)	P (mm)	$\sigma_P$ (mm)
NCEP-MM5 1993	18.7	6.7	165.3	286.88
AOGCM-MM5 “1993”	20.9	6.9	261.92	538.4
F test for variances		0.965		0.081

the RRTM radiation package (Fig. 11a–c), while these same alternative model components contribute individually to lower temperature change projections over the Great lakes Region and the Rocky Mountains. The analysis implies that in the lower Mississippi and a part of the Ohio Valley, the Betts–Miller convection scheme alone explains the warmer temperature change projections of the MIBR experiment. Synergistic effects are generally the negative of the component effects (Fig. 11d). In the positive areas in Fig. 11d (western Rockies and eastern USA), warming is a consequence of the three components interacting and not of any single component. For the Southern Plains, greater warming is consistent with decreases in precipitation frequency caused by replacing the Grell cumulus scheme with the Betts–Miller scheme (Fig. 11b). However, additional contributions to the warming result from changing the boundary layer scheme from Eta to MRF (Fig. 11a) and changing the radiation package from CCM2 to RRTM (Fig. 11c). In the simulation where all three changes act synergistically, additional surface warming encourages greater precipitation from the substitution of Betts–Miller for Grell, which leads to a combined (synergistic) cooling effect in that region (Fig. 11d).

#### 4.3 Sensitivity tests

The eight MM5 simulations listed in Table 1 were repeated for JJA 1993, substituting NCEP reanalysis forcing for the GISS AOGCM forcing used in the original set of experiments. Note that SST and atmospheric conditions designated JJA 1993 in the AOGCM simulation are from a long continuous simulation and therefore did not necessarily capture climate anomalies that were featured in the NCEP reanalysis for JJA 1993. Again, MIBR and EGC in the NCEP simulations were the warmest (wettest) and coolest (driest) respectively (not shown).

Table 5 shows a statistical comparison of the reanalysis forced simulations for JJA 1993 with the original ones based on AOGCM forcing over the continental USA. Spatial means and spatial standard deviations about those means of hourly surface air temperature were calculated for each of the eight model experiments over all land points. Spatial means and the spatial standard deviations were also computed for the simulated JJA 1993 precipitation accumulations. Means of results

**Table 6** Same as Table 5, but for the MM5 EBR simulations of JJA 1993–1997 compared with MM5 EBR simulations from the remaining five JJA seasons in the 1990s

Model	T (°C)	$\sigma_T$ (°C)	P (mm)	$\sigma_P$ (mm)
EBR 1993–1997	20.9	6.4	313.7	482.9
EBR other years	21.2	6.5	323.4	527.2
F test for variances		0.979		0.953

**Table 7** Statistical comparison of results from MIBR and EGC over the eastern USA (30–45° N and 95–75° W) for JJA 1993–1997 simulated mean temperatures and precipitation accumulations, computed on the 108 km grid and the 36 km grid

Model	T (°C)	$\sigma_T$ (°C)	P (mm)	$\sigma_P$ (mm)
MIBR 108 km	25.5	5.4	411.6	362.7
MIBR 36 km	25.0	5.4	420.2	369.2
F test for variances		0.988		0.737
EGC 108 km	19.1	4.0	224.4	335.4
EGC 36 km	18.8	4.1	260.8	272.2
P of F test for variances		0.91		0.77

over the eight versions are called here “ensemble averages.” Table 5 compares the JJA 1993 ensemble averages of the means and standard deviations for the two sets of simulations. Note that the average reanalysis forced simulation was both cooler and less rainy than the average AOGCM-forced simulation. Table 5 shows that the JJA ensemble spatial standard deviations of surface temperatures for the two sets of simulations were almost identical. According to an “*F*-test” there is a 97% probability that the variances of hourly surface temperature produced by the two sets of experiments at all land locations represent the same statistical population. On the other hand, the ensemble average spatial means and standard deviations of JJA 1993 precipitation accumulations are quite different for the two sets, and the *F*-test gives a near zero probability that the variances belong to the same statistical population. The considerably larger standard deviation of precipitation resulted from the simulation of very high JJA precipitation totals at a number of locations within the AOGCM forced experiment.

How representative are the JJA 1993–1997 simulation results? We compared the EBR results for JJA 1993–1997 to EBR simulations for the remaining five summers within the 1990s using the same statistical approach. According to Table 6, the statistics of these two sets are similar enough to conclude that the results presented here for JJA 1993–1997 are reasonably representative of the entire decade.

Mesoscale models are more commonly used for impact studies at grid spacings less than 50 km. Is the range of results on the 108 km grid representative of higher spatial resolution simulations? This was tested in a comparison of MIBR and EGC versions for JJA 1993–97. The original simulations of eastern US JJA climates were repeated, but this time on a 108/36 km nested domain (Fig. 1). Results of the experiments on the 36 km grid were compared to corresponding results on the 108 km grid within the area bounded by 30–45° N and 95–75° W. Table 7 shows that for both the MIBR and EGC model versions, the temperatures generated at both horizontal resolutions had similar means and standard deviations, and the variances have 99% and 91% probabilities, respectively, of representing the same population. Regarding the simulated precipitation, however, there is a lower probability that the variances represent the same population.

## 5 Discussion and conclusions

This study highlights MM5 sensitivity to model physics configuration for both present climate and greenhouse-gas induced climate change. The study was conducted using

the Mesoscale Modeling System Version 5 (MM5) one-way nested to the Goddard Institute for Space Studies Global Climate Model (GISS). The nested model was run on a horizontal grid with 108 km spacing for five summers (JJA) during the decades of the 1990s and 2050s (downscaling the IPCC SRES A2 Scenario) over the continental USA. Simulations with the various model configurations tested the impact of choice of boundary layer scheme, choice of cumulus parameterization, and choice of radiation package on simulation results. A wide range of model results were produced which showed the relative importance of the cumulus parameterization on both contemporary and future climate. Lesser, but still important impacts were obtained for the choice of boundary layer scheme and radiation package. Synergistic contributions, reflecting the interaction between alternative model physics components, were found to be quite important in simulating surface warming over the eastern USA. MM5 projections of surface temperature changes were not very sensitive to model configuration. Consequently, the ensemble mean temperature change “signal” reflects a consensus, averaging  $+2.8^{\circ}\text{C}$  in the western USA and  $+2.3^{\circ}\text{C}$  in the eastern USA. Changes in MM5 precipitation were, however, rather sensitive to model configuration, implying a greater uncertainty in those projections. Larger synergistic impacts on precipitation apparently lead to greater variability of simulated precipitation between the eight model versions.

The study demonstrates that boundary conditions from the GISS AOGCM have only a small impact on the sensitivity of surface temperatures to model configuration, but they may have introduced an unrealistic sensitivity of the MM5 simulated precipitation to model configuration. Some of the differences in simulated precipitation accumulations caused by substituting reanalysis boundary data for AOGCM boundary data may have, in turn, caused cooler surface air temperatures, since the characteristics of models’ precipitation do have a strong impact on modeled temperatures (Lynn et al. 2006). However, the present study found that the eight-model ensemble populations of simulated temperatures generated by boundary data from the two alternative sources are not statistically different from each other. This may be because the excess rainfall in the MM5 simulations forced by AOGCM data was more intermittent, even if it was heavy convective rain, which affects surface temperatures less than frequent rainfall at lower rates.

Han and Roads (2004) emphasized that large differences in simulated surface temperatures and precipitation generated alternatively by their GCM versus their GCM regionally forced mesoscale model resulted from model physics differences. The current study confirms the strong dependence of simulated climate characteristics on particular choices of model physics components.

Giorgi (2006) wrote: “end users of the climate change information [must be] aware of the uncertainties and limitations underlying current predictions of climate change.” He suggests that a prediction is deemed to be more reliable if different models agree on the magnitude and sign of the predicted changes. The simulated changes in surface temperatures described here were therefore more credible than the corresponding simulated changes in precipitation. Yet, our histogram analysis of simulated 2050s surface temperatures still raises an important issue. The range of mean (western and Eastern USA) surface temperatures and precipitation within the ensemble of eight model configurations was quite large. In fact, the coolest model configuration in the 2050s was not even as warm as the warmest simulation in the 1990s.

Accordingly, applications using model projections for health, agriculture, hydrology and air pollution studies need to consider that simulated surface temperatures, precipitation, boundary layer heights, and radiation budget are apt to be sensitive to the choice of model physics configuration in regional scale climate models.

**Acknowledgements** This research was supported by Grant R828733 from the U.S. Environmental Protection Agency’s Science to Achieve Results (STAR) program, NSF Grant ATM-0652518, NASA Grant NNX07AI93G and the NASA Climate Variability and Climate Change Programs. It was part of a broader program within the Climate Impacts Group of the NASA Goddard Institute for Space Studies. We thank Drs. Filippo Giorgi, Hann-Ming Henry Juang, Mike Iacono and three anonymous reviewers for their helpful comments.

**Disclaimer** Although the research described in the article has been funded wholly or in part by the US Environmental Protection Agency’s STAR program through grant R8228733, it has not been subjected to any EPA review and therefore does not necessarily reflect the views of the Agency, and no official endorsement should be inferred.

### Appendix: Factor separation analysis according to Stein and Alpert (1993)

Equations 1, 2, 3, 4, 5, 6, 7, and 8 describe the factor separation technique applied to the model simulations.

$$f'_0 = f_0 \quad (1)$$

$$f'_1 = f_1 - f_0 \quad (2)$$

$$f'_2 = f_2 - f_0 \quad (3)$$

$$f'_3 = f_3 - f_0 \quad (4)$$

$$f'_{12} = f_{12} - (f_1 - f_2) + f_0 \quad (5)$$

$$f'_{13} = f_{13} - (f_1 + f_2) + f_0 \quad (6)$$

$$f'_{23} = f_{23} - (f_2 + f_3) + f_0 \quad (7)$$

$$f'_{123} = f_{123} - (f_{12} + f_{13} + f_{23}) + (f_1 + f_2 + f_3) - f_0 \quad (8)$$

MIBR was chosen as the “base” simulation, so results (t2 or Pr) for MIBR are designated  $f_0$ , as in Eq. 1. In each equation (Eqs. 2, 3, 4, 5, 6, 7, and 8), the left hand side represents the effect on a selected model output variable of changing one or

more model parameterizations, which are referred to here as factors. The simulated output variables considered in this study are 2 m temperature ( $t_2$ ) and precipitation rate (Pr) and the factors are the choice of PBL, choice of cumulus convection scheme and choice of radiation transfer scheme. Refer to Table 1 for the definitions of the eight model configuration experiments, which include changing single factors (e.g., EBR), two factors (e.g., EGR), or all three factors (e.g., EGC). Changes in  $t_2$  or Pr resulting from changing either the PBL scheme, the cumulus convection scheme or the radiation transfer scheme are computed as  $f'_1$ ,  $f'_2$  and  $f'_3$ , respectively from Eqs. 2, 3 and 4, where  $f_1$  is the simulated  $t_2$  or Pr from EBR;  $f_2$  is the simulated  $t_2$  or Pr from MIGR;  $f_3$  is the simulated  $t_2$  or Pr from MIBC. Equations 5, 6, and 7 compute the coupled influences resulting from changing two factors at a time and Eq. 8 computes the synergistic effects of changing all three factors.

## References

- Bates GT, Giorgi F, Hostetler S (1993) Toward the simulation of the effects of the great lakes on regional climate. *Mon Weather Rev* 121:1373–1387
- Bell L, Sloan L, Snyder M (2004) Regional changes in extreme climate events: a future climate scenario. *J Climate* 17:81–87
- Bell M, Goldberg R, Hogrefe C, Kinney P, Knowlton K, Lynn B, Rosenthal J, Rosenzweig C, Patz J (2007) Climate change, ambient ozone, and health in 50 U.S. cities. *Clim Change* 82:61–76
- Betts A (1986) A new convective adjustment scheme. Part I: observational and theoretical basis. *Quart J Roy Meteor Soc* 112:677–692
- Betts A, Miller M (1986) A new convective adjustment scheme. Part II: single column tests using GATE wave, BOMEX, ATEX and Arctic air-mass data sets. *Quart J Roy Meteor Soc* 112:693–709
- Betts A, Miller M (1993) The Betts–Miller scheme. In: Emanuel KA, Raymond DJ (eds) *The representation of cumulus convection in numerical models of the atmosphere*. *Am Meteorol Soc Meteor Monogr*, vol 24, no 46. American Meteorological Society, Boston, MA, pp 107–121
- Chen F, Co-authors (1996) Modeling of land-surface evaporation by four schemes and comparison with FIFE observations. *J Geophys Res* 101:7251–7268
- Chen F, Dudhia J (2001a) Coupling an advanced land-surface/hydrology model with the Penn State/NCAR MM5 modeling system. Part I: model implementation and sensitivity. *Mon Weather Rev* 129:569–585
- Chen F, Dudhia J (2001b) Coupling an advanced land-surface/hydrology model with the Penn State/NCAR MM5 modeling system. Part II: preliminary model validation. *Mon Weather Rev* 129:587–604
- Colle B, Mass C, Westrick K (2000) MM5 precipitation verification over the Pacific Northwest during the 1997/99 cool seasons. *Weather Forecast* 15:730–744
- Cortinas J, Stensrud D (1995) The importance of understanding mesoscale model parameterization schemes for weather forecasting. *Weather Forecast* 10:716–740
- Darnell W, Staylor W, Ritchey N, Gupta S, Wilber A (1996) Surface radiation budget: a long-term global dataset of shortwave and longwave fluxes. *EOS Transactions, Electronic Supplement*. [http://www.agu.org/eos\\_elec/95206e.html](http://www.agu.org/eos_elec/95206e.html)
- Davies HC, Turner RE (1977) Updating prediction models by dynamical relaxation: an examination of the technique. *Quart J Roy Meteor Soc* 103:225–245
- Dickinson R, Errico R, Giorgi F, Bates G (1989) A regional climate model for the Western United States. *Clim Change* 15:383–422
- Diffenbaugh N, Pal J, Trapp R, Giorgi F (2005) Fine-scale processes regulate the response of extreme events to global climate change. *Proc Nat'l Acad Sci U S A* 102:15774–15778
- Dudhia J (1993) A non-hydrostatic version of the Penn State/NCAR mesoscale model: validation tests and simulation of an Atlantic cyclone and cold front. *Mon Weather Rev* 121:1493–1513
- Fu C, Wang S, Xiong Z, Gutowski W, Lee D-K, McGregor J, Sato Y, Kato H, Kim J-W, Suh M-S (2005) Regional climate model intercomparison project for Asia. *Bull Am Meteorol Soc* 86:257–266

- Gao X, Pal J, Giorgi F (2006) Projected changes in mean and extreme precipitation over the Mediterranean region from a high resolution double nested RCM simulation. *Geophys Res Lett* 33:LO3706. doi:[10.1029/2005GL024954](https://doi.org/10.1029/2005GL024954)
- Giorgi F (2006) Climate change prediction. *Clim Change* 73:239–265
- Giorgi F, Marinucci M (1996) An investigation of the sensitivity of simulated precipitation to model resolution and its implications for climate studies. *Mon Weather Rev* 124:148–156
- Giorgi F, Marinucci M, Bates G (1993a) Development of a second-generation regional climate model (RegCM2). Part I: boundary-layer and radiative transfer processes. *Mon Weather Rev* 121:2794–2813
- Giorgi F, Marinucci M, Bates G, De Canio G (1993b) Development of a second-generation regional climate model (RegCM2). Part II: convective processes and assimilation of lateral boundary conditions. *Mon Weather Rev* 121:2814–2832
- Giorgi F, Brodeur C, Bates G (1994) Regional climate change scenarios over the United States produced with a nested regional climate model: spatial and seasonal characteristics. *J Climate* 7:375–399
- Grell G (1993) Prognostic evaluation of assumptions used by cumulus parameterizations. *Mon Weather Rev* 121:764–787
- Grell G, Kuo Y-H, Pasch R (1991) Semi-prognostic tests of cumulus parameterization schemes in the middle latitudes. *Mon Weather Rev* 119:5–31
- Grell G, Dudhia J, Stauffer D (1994) A description of the fifth-generation Penn State/NCAR mesoscale model (MM5). NCAR Technical Note NCAR/TN-298+STR, 117 pp
- Hack JJ, Boville BA, Breigleb BP, Kiehl JT, Rasch PJ, Williamson DL (1993) Description of the NCAR Community Climate Model (CCM2). NCAR Technical Note NCAR/TN-382+STR, 120 pp
- Han J, Roads J (2004) U.S. Climate sensitivity simulated with the NCEP regional spectral model. *Clim Change* 62:115–154
- Hansen J, Co-authors (2002) Climate forcings in Goddard Institute for space studies SI2000 simulations. *J Geophys Res* 107:4347. doi:[10.1029/2001JD001143](https://doi.org/10.1029/2001JD001143)
- Hogrefe C, Biswas J, Lynn B, Civerolo K, Ku J-Y, Rosenthal J, Rosenzweig C, Goldberg R, Kinney P (2004) Simulating regional-scale ozone climatology over the eastern United States: model evaluation results. *Atmos Environ* 38:2627–2638. doi:[10.1016/j.atmosenv.2004.02.033](https://doi.org/10.1016/j.atmosenv.2004.02.033)
- Hong S-Y, Pan H-L (1996) Non-local boundary layer vertical diffusion in a medium-range forecast model. *Mon Weather Rev* 124:2322–2339
- Intergovernmental Panel on Climate Change (2000) In: Nakicenovic N (ed) Special report on emissions scenarios. Cambridge University Press, Cambridge
- Jacquemin B, Noilhan J (1990) Sensitivity study and validation of a land surface parameterization using the HAPEX-MOBILHY data set. *Boundary-Layer Meteorol* 52:93–134
- Janjic Z (1990) The step-mountain coordinate: physical package. *Mon Weather Rev* 118:1429–1443
- Janjic Z (1994) The step-mountain Eta coordinate model: further development of the convection, viscous sublayer, and turbulent closure schemes. *Mon Weather Rev* 122:927–945
- Knowlton K, Rosenthal J, Hogrefe C, Lynn B, Gaffin S, Goldberg R, Rosenzweig C, Civerolo K, Ku J-Y, Kinney P (2004) Assessing ozone-related health impacts under a changing climate. *Environ Health Perspect* 112:1557–1563
- Leung L, Qian Y (2003) The sensitivity of precipitation and snowpack simulations to model resolution via nesting in regions of complex terrain. *J Hydrometeorol* 4:1025–1043
- Leung L, Qian Y, Han J, Roads J (2003a) Intercomparison of global reanalysis and regional simulations of cold season water budgets in the Western United States. *J Hydrometeorol* 4:1067–1087
- Leung L, Qian Y, Bian X (2003b) Hydroclimate of the Western United States based on observations and regional climate simulations of 1981–2000. Part I: seasonal statistics. *J Climate* 16:1892–1911
- Leung L, Qian Y, Bian X, Hunt A (2003c) Hydroclimate of the Western United States based on observations and regional climate simulations of 1981–2000. Part II: mesoscale ENSO anomalies. *J Climate* 16:1912–1928
- Leung L, Qian Y, Bian X, Washington W, Han J, Roads J (2004) Mid-century ensemble regional climate change scenarios for the Western United States. *Clim Change* 62:75–113
- Liang X-Z, Li L, Kunkel K (2004) Regional climate model simulation of U.S. precipitation during 1982–2002. Part I: annual cycle. *J Climate* 17:3510–3529
- Lynn B, Druryan L, Hogrefe C, Dudhia J, Rosenzweig C, Goldberg R, Rind D, Healy R, Kinney P, Rosenthal J (2004) Sensitivity of present and future surface temperatures to precipitation characteristics. *Climate Res* 28:53–65
- Lynn B, Healy R, Druryan L (2006) An analysis of the potential for extreme temperature change based on observations and model simulations. *J Climate* 20:1539–1554

- Mahrt L, Ek M (1984) The influence of atmospheric stability on potential evaporation. *J Climate Appl Meteor* 23:222–234
- Mahrt L, Pan H (1984) A two-layer model of soil hydrology. *Bound-Layer Meteor* 29:1–20
- Mass C, Ovens D, Westrick K, Colle B (2002) Does increasing horizontal resolution produce better forecasts? The results of two years of real-time numerical weather prediction over the Pacific Northwest. *Bull Am Meteorol Soc* 82:407–430
- Mlawer E, Taubman S, Brown P, Iacono M, Clough S (1997) Radiative transfer for inhomogeneous atmosphere: RRTM, a validated correlated-k model for the longwave. *J Geophys Res* 102:16663–16682
- Nobre P, Moura A, Sun L (2001) Dynamical downscaling of seasonal climate prediction over Nordeste Brazil with ECHAM3 and NCEP's regional spectral models at IRI. *Bull Am Meteorol Soc* 82:2787–2796
- Noilhan J, Planton S (1989) A simple parameterization of land surface processes for meteorological models. *Mon Weather Rev* 117:536–549
- Pan H-L, Mahrt L (1987) Interaction between soil hydrology and boundary-layer development. *Boundary-Layer Meteorol* 38:185–202
- Rosenzweig C, Solecki W (Eds) (2001) Climate change and a global city: the potential consequences of climate variability and change—Metro East Coast. Report for the US Global Change Research Program, National Assessment of the Potential Consequences of Climate Variability and Change for the United States. Report. Columbia Earth Institute, Columbia University, New York, NY
- Russell G, Miller J, Rind D (1995) A coupled atmosphere-ocean model for transient climate change studies. *Atmos Ocean* 33:683–730
- Sato M, Hansen J, McCormick M, Pollack J (1993) Stratospheric aerosol optical depth, 1850–1990. *J Geophys Res* 98:22987–22994
- Stein U, Alpert P (1993) Factor separation in numerical simulations. *J Atmos Sci* 50:2107–2115
- Walsh K, McGregor J (1995) January and July climate simulations over the Australian region using a limited-area model. *J Climate* 8:2387–2403
- Yang Z, Arritt R (2002) Tests of a perturbed physics ensemble approach for regional climate modeling. *J Climate* 15:2881–2896